



**HAL**  
open science

## Electrochemical studies of CO<sub>2</sub>-reducing metalloenzymes

Marta Meneghello, Christophe Léger, Vincent Fourmond

► **To cite this version:**

Marta Meneghello, Christophe Léger, Vincent Fourmond. Electrochemical studies of CO<sub>2</sub>-reducing metalloenzymes. *Chemistry - A European Journal*, 2021, 10.1002/chem.202102702 . hal-03358088

**HAL Id: hal-03358088**

**<https://hal.science/hal-03358088>**

Submitted on 29 Sep 2021

**HAL** is a multi-disciplinary open access archive for the deposit and dissemination of scientific research documents, whether they are published or not. The documents may come from teaching and research institutions in France or abroad, or from public or private research centers.

L'archive ouverte pluridisciplinaire **HAL**, est destinée au dépôt et à la diffusion de documents scientifiques de niveau recherche, publiés ou non, émanant des établissements d'enseignement et de recherche français ou étrangers, des laboratoires publics ou privés.

# Electrochemical studies of CO<sub>2</sub>-reducing metalloenzymes

Marta Meneghello, Christophe Léger, Vincent Fourmond\*

*CNRS, Aix-Marseille Université, Laboratoire de Bioénergétique et Ingénierie des Protéines, UMR 7281, Institut de Microbiologie de la Méditerranée, and Institut Microbiologie, Bioénergies et Biotechnologie, 31 chemin J. Aiguier, F-13402 Marseille cedex 20, France*

\*e-mail: [vincent.fourmond@imm.cnrs.fr](mailto:vincent.fourmond@imm.cnrs.fr)

@BIP6\_Marseille

## Abstract

Only two enzymes are capable of directly reducing CO<sub>2</sub>: the CO dehydrogenase, which produces CO at a [NiFe<sub>4</sub>S<sub>4</sub>] active site, and the formate dehydrogenase, which produces formate at a mononuclear W or Mo active site. Both metalloenzymes are very rapid, energy-efficient and specific in terms of product. They have been connected to electrodes with two different objectives. A series of studies used protein film electrochemistry to learn about different aspects of the mechanism of these enzymes (reactivity with substrates, inhibitors...). Another series focused on taking advantage of the catalytic performance of these enzymes to build biotechnological devices, from CO<sub>2</sub>-reducing electrodes to full photochemical devices performing artificial photosynthesis. Here, we review all these works.

Marta Meneghello obtained her Ph.D. in Chemistry from the University of Southampton (UK) in 2018, under the supervision of Prof P.N. Bartlett, working on the immobilization of redox enzymes at electrode surfaces. Since 2018, she is a postdoctoral researcher in the group of Christophe Léger and Vincent Fourmond at the CNRS of Marseille (France). Her current research focuses on kinetics studies of metalloenzymes, such as CO dehydrogenase and formate dehydrogenase, using electrochemical methods.



Dr Christophe Léger obtained his Ph.D. from the University of Bordeaux and was a postdoc in the group of Fraser Armstrong from 1999 to 2002. He is “Directeur de Recherche” at CNRS. His interests lie in kinetic and mechanistic studies of complex metalloenzymes.

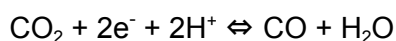


Vincent Fourmond obtained his Ph.D. at the interface of physics and biology from Université Paris Diderot in 2007. He held postdoctoral positions first in the group of Christophe Léger in Marseille and then Vincent Artero in Grenoble, before coming back to Marseille as a permanent CNRS researcher in 2011. His research interests revolve around the use of kinetic techniques, principally protein film electrochemistry, to understand the mechanisms of metalloenzymes (hydrogenases, CO dehydrogenases, molybdenum enzymes), the development of methodological aspects of PFE, and the development and maintenance of the open source data analysis software QSoas<sup>[1]</sup>.



## Introduction

The assimilation of carbon is a central process in biology, since the carbon of living organisms originates from the biological fixation of CO<sub>2</sub>. There are at least six pathways for the assimilation of carbon<sup>[2,3]</sup>, among which the most important in terms of biomass production is the Calvin cycle, featuring the Ribulose-1,5-bisphosphate carboxylase-oxygenase (Rubisco), which catalyzes the (non-redox) carboxylation of ribulose<sup>[4]</sup>, as the entry point of CO<sub>2</sub>. Most of these pathways are cyclic, featuring core carbon compounds of small size that get carboxylated, reduced, and eventually split back into the original compounds. Some of these carboxylations are reductive carboxylations, like in the case of the reaction catalyzed by pyruvate:ferredoxin oxidoreductase, which produces pyruvate from acetyl-CoA and CO<sub>2</sub>.<sup>[5,6]</sup> Only two enzymes are known to catalyze the *direct reduction* of CO<sub>2</sub>: CO dehydrogenase (CODH), which catalyzes the reduction of CO<sub>2</sub> to CO:



and formate dehydrogenase (FDH), which catalyzes the reduction of CO<sub>2</sub> to formate:



Both of them participate in the Wood-Ljungdahl pathway, a major CO<sub>2</sub> fixation pathway in anaerobic organisms<sup>[7]</sup>, which is linear rather than cyclic.

CODH and FDH have attracted considerable interest in the past decades, owing to their outstanding catalytic performance. Both enzymes function “reversibly”<sup>[8,9]</sup>, which means that they catalyze their respective reactions at high rates even when very small thermodynamic driving forces are applied<sup>[10]</sup>. This makes them very attractive in the context of energy storage, in which energy efficiency is a fundamental requirement. They are also very active, with turnover rates of up to 4×10<sup>4</sup> s<sup>-1</sup> reported for CODH<sup>[11]</sup>. Finally, they are very specific in terms of product: while man-made catalysts tend to produce a mixture of reduced carbon compounds (CO, formate, oxalate, etc...) and even H<sub>2</sub>, FDH and CODH give no by-products. It is thought that these enzymes could help us store energy in the form of carbonaceous fuels<sup>[6]</sup>, either by studying them to understand the origin of their performance, or by directly using them as catalysts.

Perhaps the most intuitive way to study or use redox enzymes is by connecting them to electrodes, driving the reactions in one direction or the other by applying appropriate electrode potentials. The use of electrochemical techniques to study the mechanism of immobilized redox enzymes is known as Protein Film Electrochemistry (PFE), which consists in measuring the catalytic current, proportional to the turnover rate, and interpreting its variations as a function of experimental conditions<sup>[10,12–15]</sup>. This approach has been used to study the effect of inhibitors, redox inactivation/reactivation, and the catalytic mechanism itself. The articles reporting on electrochemical studies involving CODH or FDH can therefore be separated in two categories: on one hand, some PFE studies take advantage of the direct connection between the electrode and the enzyme to learn more about the enzyme, and to better understand the origins of their catalytic properties. On the other hand, the enzymes are directly used in biotechnological devices for the reduction of CO<sub>2</sub>. In the present manuscript, we review both types of studies.

## CO dehydrogenases

CO dehydrogenases are metalloenzymes that catalyze the oxidation of CO to CO<sub>2</sub>. This function regroups two classes of phylogenetically unrelated enzymes. The first one, called the MoCu CODH, is found in aerobic carboxidotrophic bacteria. They are characterized by an active site containing both molybdenum and copper; they belong to the same superfamily of molybdenum/tungsten enzymes as the formate dehydrogenase<sup>[16,17]</sup>. They only catalyze the oxidation of CO, not the reverse reaction, and they have not been studied using electrochemical techniques so far.

The second class is that of the nickel CODHs, which catalyze the bidirectional and reversible<sup>[10]</sup> reduction of CO<sub>2</sub> to CO at a [NiFe<sub>4</sub>S<sub>4</sub>] active site<sup>[18]</sup>. Most of the Ni CODHs characterized so far (and all of those that have been connected to an electrode) present an overall structure resembling that of *Carboxydotherrmus hydrogenoformans* (*Ch*) CODH II, shown in figure 1 (left). The structure is a homodimer containing a total of 5 metallic clusters: two B clusters, which are classical [4Fe4S] clusters; two C clusters, which are the [NiFe<sub>4</sub>S<sub>4</sub>] active sites; and a single D cluster located at the interface between the two monomers, which can either be a [4Fe4S] or a [2Fe2S] cluster<sup>[19–21]</sup>. CODHs are sometimes associated<sup>[19–21]</sup> with an acetyl-CoA synthase subunit (ACS) to form a bifunctional ACS/CODH complex, which can reduce CO<sub>2</sub> to CO and directly combine it with a methyl group to form an acetyl-CoA moiety. The most studied of these

ACS/CODH complexes is that of *Moorella thermoacetica*<sup>[18,22]</sup>; to date, no ACS/CODH complex has been directly connected to an electrode.

Ni CODHs are found almost only in anaerobic bacteria/archaea<sup>[23]</sup> where they play different roles, such as generation of reducing equivalents for the cell metabolism (NAD(P)H), carbon assimilation (coupled with the ACS) in the Wood-Ljungdahl pathway<sup>[7]</sup>, respiration on CO/H<sup>+</sup> (coupled with a membrane-bound hydrogenase)<sup>[24,25]</sup>, defence against oxidative stress<sup>[24,26]</sup>, or CO detoxification<sup>[27]</sup>, and probably other, yet unknown, biological functions<sup>[28]</sup>.

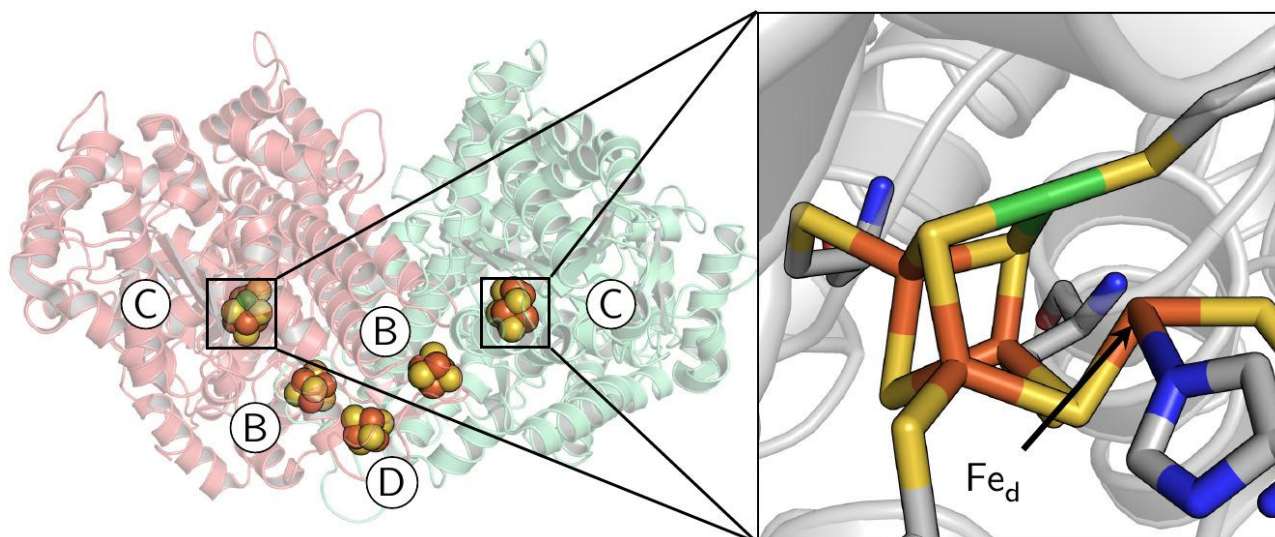


Figure 1: left: overall structure of *Ch* CODH II, which is representative of all the Ni CODHs that have been studied so far in electrochemistry; the metallic clusters are represented as spheres<sup>[29]</sup>. Right: zoom onto the [NiFe<sub>4</sub>S<sub>4</sub>] active site (C cluster), represented as sticks along with the direct ligands. Color code for the inorganic elements: Fe (orange), Ni (green), S (yellow). The “dangling” iron is indicated as Fe<sub>d</sub>. PDB used: 1SU8<sup>[30]</sup>.

The active site “C cluster” is shown in figure 1 (right). It consists of a [NiFe<sub>3</sub>S<sub>4</sub>] moiety arranged in a slightly distorted cubane connected *via* one of the S<sup>2-</sup> ligands to a “dangling” Fe ion (designated by Fe<sub>d</sub> in figure 1). Three different redox states have been identified by spectroscopic approaches: a C<sub>ox</sub> state, which is thought to be an oxidized, inactive state of the enzyme; a C<sub>red1</sub> state, thought to be the one competent for binding of CO; and a C<sub>red2</sub> state, which is 2-electron more reduced than C<sub>red1</sub> and is thought to bind CO<sub>2</sub><sup>[18]</sup>. The current mechanistic propositions all feature C<sub>red1</sub> and C<sub>red2</sub> as intermediates (and exclude C<sub>ox</sub>).

In the C<sub>red1</sub> state, a OH<sup>-</sup> ligand completes the coordination sphere of the dangling iron. Jeoung and Dobbek could obtain the crystal structure of CO<sub>2</sub>-bound CODH in the redox conditions which favor the accumulation of C<sub>red2</sub><sup>[29]</sup>. They found that CO<sub>2</sub> binds as a μ<sub>2</sub>η<sub>2</sub> ligand, with the C atom coordinating the Ni ion and one of the O atoms coordinated to the dangling iron. Proposed mechanisms agree about the fact that CO binds the oxidized C<sub>red1</sub> state<sup>[31]</sup>; a bond is created between the C atom and the OH<sup>-</sup> ligand on the dangling Fe, which leads to the formation of the CO<sub>2</sub>-bound state. What happens next is less consensual. Some advocate for the formation of a “Ni(0)” reduced intermediate after departure of CO<sub>2</sub> from the active site<sup>[29]</sup>, while others have proposed the formation of a nickel hydride species<sup>[32]</sup>. However, a recent thorough DFT investigation by Breglia and coworkers questions the latter hypothesis<sup>[33]</sup>.

Most of the CODHs connected so far to electrodes for PFE studies were simply adsorbed to bare pyrolytic graphite edge electrodes (*Carboxydotherrmus hydrogenoformans* CODH I & II, *Desulfovibrio vulgaris* CODH, *Thermococcus sp. AM4* CODH 1 & 2), with the exceptions of *Ch* CODH IV, which required neomycin as co-adsorbant<sup>[26]</sup>, and *Rhodospirillum rubrum* CODH, which was immobilized on functionalized carbon nanotubes<sup>[34]</sup>.

## Reactivity of CODH with its substrates

One of the simplest experiments to perform with enzymes immobilized on electrodes is to determine the value of their Michaelis constant ( $K_m$ ). This is easy with gaseous substrates, because one can take advantage of the spontaneous decrease in substrate concentration over time due to the exchange of gas between the electrochemical solution and the gas phase above it. When the cell is fully open, in a glove box for instance, this exchange results in the exponential decrease over time of the concentration of dissolved gas<sup>[35]</sup> (see panel a in figure 2). This strategy allows the exploration of a large range of concentrations in an experiment that consists in a single injection of substrate-saturated solution to the electrochemical cell. Figure 2 shows two examples of such experiments: the determination of the  $K_m$  for CO of *Ch* CODH IV (panel b), and the determination of the  $K_m$  for CO<sub>2</sub> of *Tc* CODH 1 (panel c). In both cases, the injection of the substrate leads to an instant increase in the magnitude of the current (positive for CO oxidation, negative for CO<sub>2</sub> reduction), followed by a slow decrease, which lasts much longer in the case of panel b, and then an acceleration of the decrease, finishing with a perfect mono-exponential decay. Appropriate modelling can be used to determine both the characteristic time of the departure of the substrate from the solution and the value of  $K_m$ <sup>[35]</sup>. In figure 2, in order to help comparing the experiments, the time is normalized by  $\tau$ , the characteristic time of departure of the gas. The values of  $K_m$  determined so far by electrochemistry are given in table 1.

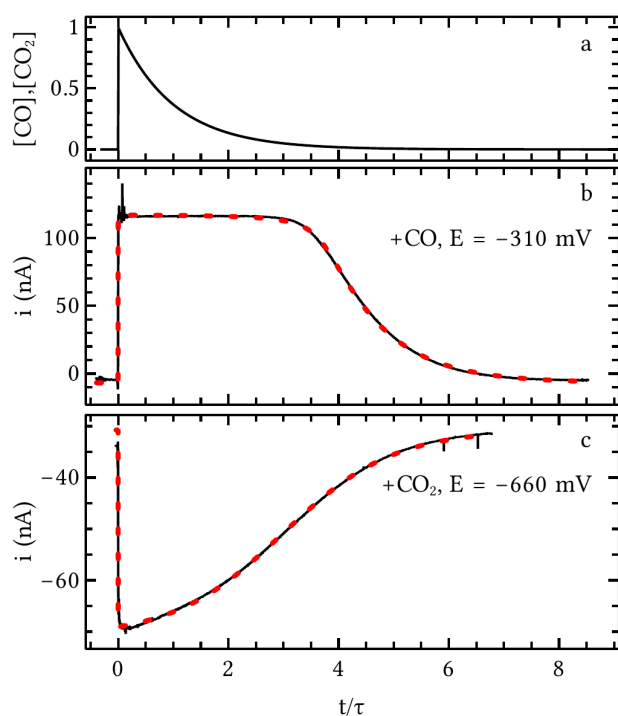


Figure 2: chronoamperometric experiments used to determine the  $K_m$  for CO and CO<sub>2</sub> of CO dehydrogenases. Panel a: evolution of the (normalized) concentration of CO or CO<sub>2</sub> over time. The time is normalized by the characteristic time of departure of CO/CO<sub>2</sub> from the solution ( $\tau$ ). Panel b: response of *Ch* CODH IV to an injection of a CO-saturated solution. The black curve is the experimental current, the red dotted curve is the fit, yielding a  $K_m$  of 48 nM<sup>[26]</sup>. Conditions: E = -310

mV vs. SHE, pH 7, T = 25 °C, injected CO: 50 µM. Data reprinted from ref. [26]. Panel c: response of *Tc* CODH 1 to an injection of CO<sub>2</sub>. The black curve is the experimental current, the red dotted curve is the fit, yielding a  $K_m$  of 0.42 mM<sup>[36]</sup>. Conditions: E = -660 mV vs. SHE, pH 6, T = 25 °C, 7 mM CO<sub>2</sub> injected. Data reprinted from ref. [36].

Enzyme	$K_m$ for CO	$K_m$ for CO <sub>2</sub>	refs
<i>Ch</i> CODH I	2 µM	7 mM, 8mM	[9,37]
<i>Ch</i> CODH II	8 µM	6 mM, 8 mM	[36]
<i>Ch</i> CODH IV	20 nM -- 800 nM	N/D	[26]
<i>Dv</i> CODH	2 µM	N/D	[38]
<i>Tc</i> CODH 1	0.3 µM	0.42 mM	[36]
<i>Tc</i> CODH 2	0.9 µM	> 7 mM	[36]

Table 1: values of  $K_m$  for CO and CO<sub>2</sub> determined using electrochemistry. The two values given for the  $K_m$  for CO<sub>2</sub> in the case of *Ch* CODH I and II correspond to two different potentials<sup>[37]</sup>.

The case of *Ch* CODH IV also demonstrates a common problem with CO dehydrogenases. These enzymes are so active that CO oxidation in an electrochemical cell is often mass-transport-limited, i.e. limited by the rate at which the rotating disc electrode pumps CO towards the electrode. Determining a reliable value of  $K_m$  requires taking into account mass-transport limitations<sup>[38]</sup>. *Ch* CODH IV is in fact a "perfect" enzyme<sup>[39]</sup>: it is so active that the solution-phase catalytic oxidation of CO is also limited by the diffusion of CO towards the enzyme, over a large range of temperature (between 25 °C and 70 °C)<sup>[26]</sup>.

Experiments relying on the exponential decrease of the concentration of dissolved gas were also employed to determine the  $K_m$  for CO<sub>2</sub> for the reductive reaction. With the exception of *Tc* CODH 1, for which a value of 0.42 mM could reliably be determined, the  $K_m$  values for CO<sub>2</sub> are very high (almost 10 mM), and hard to determine precisely. In some cases, like *Tc* CODH 2, it was only possible to provide a lower value<sup>[36]</sup>.

Product inhibition can also be probed using similar experiments, injecting first the substrate and then the product: a decrease in magnitude of the current after the injection of the product is indicative of product inhibition. To the best of our knowledge, no inhibition of CO oxidation by CO<sub>2</sub> was ever observed. However, the reduction of CO<sub>2</sub> by CODHs is generally inhibited by the presence of CO. For *Ch* CODH I, Wang and coworkers found an inhibition constant of 46 µM or 337 µM depending on the applied potential<sup>[40]</sup>. We determined inhibition constants of 0.36 µM and 22 µM for *Tc* CODH 1 and 2, respectively<sup>[36]</sup>.

## Inhibition of CODHs by O<sub>2</sub>

CODHs have a reputation for being "extremely O<sub>2</sub>-sensitive", as was written by Can and coworkers in 2014<sup>[18]</sup>. However, before 2015, this reputation was based on very little published data. Two independent studies published in 2015 reported on the inhibition of *Ch* CODH II<sup>[41,42]</sup> and *Dv* CODH<sup>[42]</sup> by O<sub>2</sub>. They both found that CODHs inactivate very quickly upon exposure to O<sub>2</sub>, but that, unexpectedly, at least a fraction of the initial activity is recovered after an exposure to very

reducing conditions. We demonstrated that at least 3 distinct species are produced upon reaction with  $O_2$ : a species that reactivates spontaneously upon departure of  $O_2$ , one that requires reduction before becoming active again, and a third one that does not reactivate<sup>[42]</sup>. The inhibition by  $O_2$  of *Ch* CODH IV<sup>[26]</sup> and of *Tc* CODH 1 & 2<sup>[36]</sup> was also characterized.

Overall, a large variety of different behaviors was observed. The bimolecular rate constant with  $O_2$  ranges from  $0.15 \text{ s}^{-1}\mu\text{M}^{-1}$  in the case of *Tc* CODH 1<sup>[36]</sup>, to more than  $10 \text{ s}^{-1}\mu\text{M}^{-1}$  for *Ch* CODH II<sup>[42]</sup>. Most of the CODHs studied so far reactivate upon reduction, but only to a small extent (around 20 % of the initial activity), with the exception of *Ch* CODH IV, which does not reactivate at all but is relatively resistant to  $O_2$ <sup>[26]</sup>, and *Dv* CODH which fully reactivates upon reduction after exposure to up to 10 % of atmospheric  $O_2$  for 30 s<sup>[42]</sup>. The molecular nature of the various species formed upon reaction with  $O_2$  have not been fully elucidated yet; however, we proposed that the inactive species that is reductively reactivated could be a form of the active site in which the nickel and dangling iron have changed position and coordination<sup>[21]</sup>.

*Dv* CODH is in fact so resistant to  $O_2$  that it is possible to purify the enzyme aerobically<sup>[43]</sup> (with only a 70 % loss of specific activity); this feature is apparently related to the nature of the D cluster of *Dv* CODH. This cluster is a [2Fe2S] cluster unlike in the other characterized CODHs, which have a [4Fe4S] cluster. Replacement of the [2Fe2S] cluster with a [4Fe4S] in *Dv* CODH led to a drastically decreased activity after aerobic purification, but almost no change in the anaerobic purified enzyme<sup>[43]</sup>.

## Other inhibitors

Inhibition of CODHs by  $CN^-$ ,  $NCO^-$ ,  $S^{2-}$ <sup>[40]</sup>, and  $N_2O$ <sup>[41]</sup> was also studied by electrochemistry.  $CN^-$  inhibits both CO oxidation and  $CO_2$  reduction, but only at high enough potentials; this was interpreted to mean that  $CN^-$  binds to the  $C_{red1}$  state of the active site<sup>[40]</sup>.  $NCO^-$  inhibits the reduction of  $CO_2$  at low potentials and has no influence on the oxidation of CO; this was interpreted to mean that it binds to the  $C_{red2}$  redox state of the active site.  $S^{2-}$  inhibits the oxidation of CO, but only at very high potentials, and displays a very complicated behaviour, with slow inhibition and rates of inhibition/reactivation apparently strongly dependent on potential. Last,  $N_2O$ , a slow alternative substrate that can be reduced by the CODH, was found to inhibit very slightly CO oxidation at low potentials<sup>[41]</sup>. Oxidative conditions themselves inhibit the enzymes, as could be observed from cyclic voltammograms with a strong hysteresis recorded with *Ch* CODH I<sup>[9]</sup> and also *Dv* CODH<sup>[44]</sup>, which are reminiscent of what was observed in the case of NiFe hydrogenases<sup>[45,46]</sup>. These voltammograms are indicative of the formation of oxidized, inactive species at high potentials, which was assigned to  $C_{ox}$ <sup>[9]</sup>, but the inactivation process has not been studied in detail so far.

## Formate dehydrogenases

Formate dehydrogenases (FDH) are enzymes that catalyze the oxidation of formate to  $CO_2$ . Two unrelated classes of enzymes correspond to this definition. The first consists in the so-called “metal-free” or “NADH-dependent” formate dehydrogenases, which do not contain metallic centers and catalyze the transfer of a hydride from formate to  $NAD^+$  or  $NADP^+$ <sup>[47]</sup>. They are not known to catalyze the reduction of  $CO_2$ .

The other class of formate dehydrogenases belongs to the superfamily of molybdenum enzymes<sup>[48]</sup>, and in particular to the Mo/W bis-PGD (pyranopterin guanosine dinucleotide) subfamily, which are omnipresent in bacteria and archaea and are involved in various cellular

functions, including nitrogen cycling, respiration, and carbon assimilation<sup>[49,50]</sup>. Enzymes from the Mo/W bis-PGD family are characterized by an active site featuring a Mo or W ion that is coordinated by two dithiolene ligands coming from pyranopterins (molybdopterin), and most often by a proteic ligand. They catalyze mostly 2-electron redox reactions like transfers of oxygen atoms or sulfur<sup>[49]</sup>. In the case of the FDH, in addition to the dithiolene ligands, the coordination sphere of the metal is completed by either a cysteine or a selenocysteine, and an inorganic sulfide that is necessary for the activity<sup>[51,52]</sup>. FDHs widely differ in terms of the other cofactors present in the structure. *Ec* FdhF contains a single [4Fe4S] cluster<sup>[53]</sup>, *Dv* FdhAB contains a [4Fe4S] cofactor in the catalytic subunit (in green in figure 3) and three other [4Fe4S] clusters in the B subunit (in cyan). *Syntrophobacter fumaroxidans* (*Sf*) FDH is thought to contain a total of 9 FeS clusters<sup>[8]</sup>.

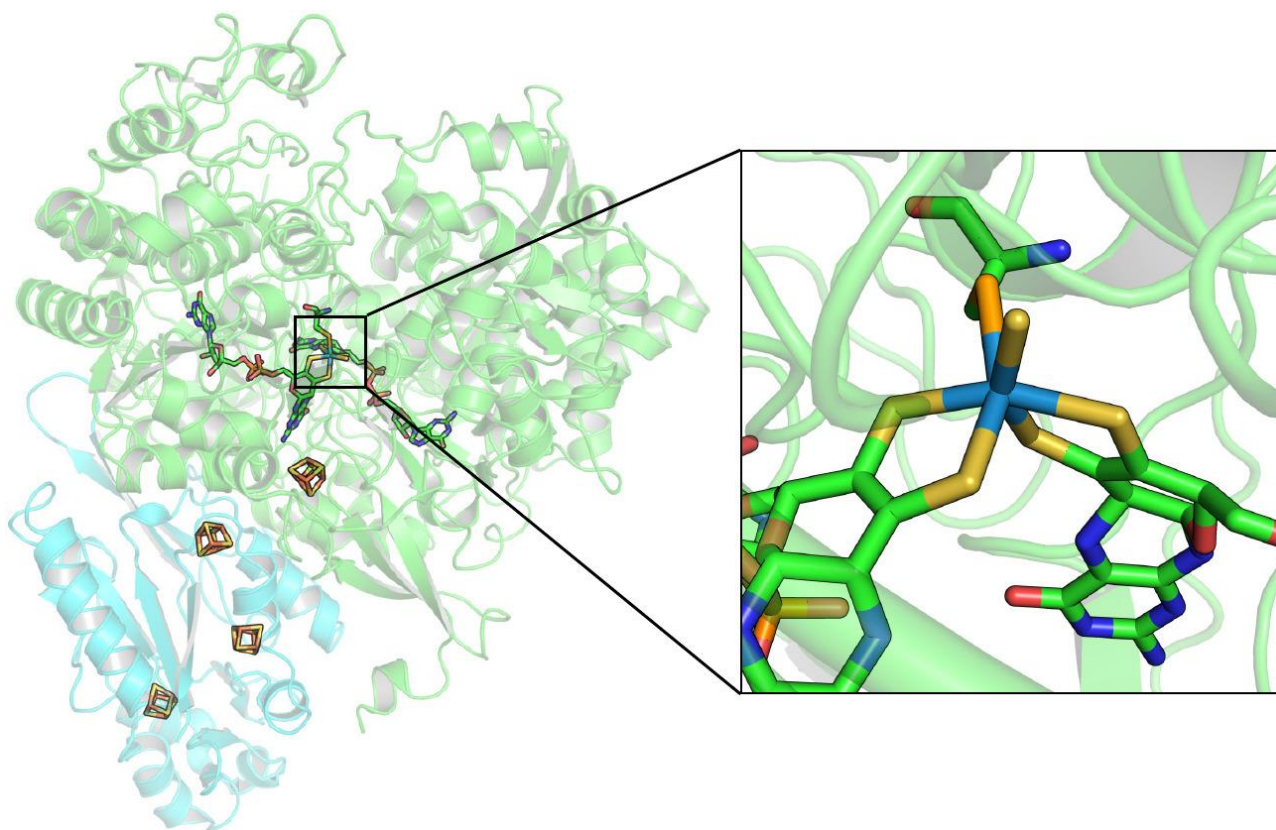


Figure 3: left: overall structure of FdhAB from *Desulfovibrio vulgaris Hildenborough*, which features a W active site (PDB: 6SDR)<sup>[54]</sup>. Right: zoom into the active site, showing the W ion (in light blue), coordinated by two dithiolene ligands from the molybdopterin, the SeCys residue and an inorganic sulfide. Color code: Fe (dark orange), S (yellow), Se (light orange), W (blue).

Considering that many of the other enzymes from the Mo/W bis-PGD family catalyze O atom transfers, it is natural to wonder about the nature of the substrate of the reduction reaction: does the FDH work by adding a hydride to CO<sub>2</sub> or by removing an O atom from HCO<sub>3</sub><sup>-</sup>? Khangulov and coworkers showed that, over a short time, the oxidation of <sup>16</sup>O-formate in <sup>18</sup>O-enriched water only gives <sup>16</sup>O-CO<sub>2</sub>, which suggests that CO<sub>2</sub> (rather than HCO<sub>3</sub><sup>-</sup>) is the product<sup>[55]</sup>. However, this method for determining the nature of the substrate is prone to artifacts if the water contained in the enzyme does not exchange quickly<sup>[56]</sup>. A strong evidence that CO<sub>2</sub> is indeed the substrate came from recent electrochemical experiments that took advantage of the relatively slow equilibration time between CO<sub>2</sub> and HCO<sub>3</sub><sup>-</sup> (about 20 s at pH 7 and 25 °C): for a short time after the injection of either CO<sub>2</sub> or HCO<sub>3</sub><sup>-</sup> (freshly prepared), only the injected species is present in solution. Injection of CO<sub>2</sub> led to the immediate appearance of a reduction current, in contrast to an injection of HCO<sub>3</sub><sup>-</sup>, showing unambiguously that CO<sub>2</sub> is the substrate for the reduction reaction<sup>[57]</sup>.

The puzzling discovery that a sulfide ligand in the coordination sphere of the Mo/W is required for catalysis<sup>[51,52]</sup> raised important questions about the catalytic mechanism. The Mo/W ion has 6 ligands, which are all S atoms; since a 7-coordinated Mo/W intermediate seems unlikely, how does formate/CO<sub>2</sub> bind to the active site? Several mechanisms have been proposed<sup>[58]</sup>, which consider either the complete decooordination of the selenocysteine ligand during the catalytic cycle<sup>[59]</sup>, the so-called “sulfur shift” mechanism by which the selenocysteine ligand moves from the first to the second coordination sphere *via* the formation of a Se-S bond to the active site sulfide<sup>[60]</sup>, or, more recently, the possibility that formate/CO<sub>2</sub> does not coordinate directly the metal but exchanges a hydride with the sulfide ligand<sup>[61,62]</sup>. The question is still open, but the recent determination of the structure of a reduced enzyme which features coordination of the SeCys-bound suggests that the full decooordination of SeCys during the catalytic cycle is unlikely<sup>[54]</sup>.

## Catalytic and non-catalytic responses

To date, four FDHs have been successfully connected to electrodes. Unlike many CODHs, which could be immobilized on bare pyrolytic graphite edge (PGE) electrodes, FDHs required more sophisticated immobilization approaches, such as graphite-epoxy electrodes for *E. coli* (*Ec*) FdhF<sup>[63]</sup>, carbon nanotubes-covered graphite electrodes for *C. necator* FDH<sup>[63,64]</sup>, ITO, TiO<sub>2</sub> or polymyxin-covered PGE electrodes for *D. vulgaris* (*Dv*) FdhAB<sup>[57,65]</sup>. Only *S. fumaroxidans* (*Sf*) FDH could successfully be connected to bare PGE electrodes<sup>[8]</sup>.

Bidirectional voltammograms were recorded for the FDHs from *Dv*, *Sf* and *Ec*. Figure 4 shows voltammograms obtained for the three enzymes under similar conditions. Although it is not possible to quantitatively compare the voltammograms, since the pH and the formate/CO<sub>2</sub> concentrations are slightly different, it is nonetheless striking that all the three enzymes have a catalytic bias<sup>[66]</sup> close to unity in this potential range. They are reversible<sup>[10]</sup> in the sense that a slight deviation from the equilibrium potential yields a significant current, maybe less so for *Dv* FDH (red trace in figure 4).

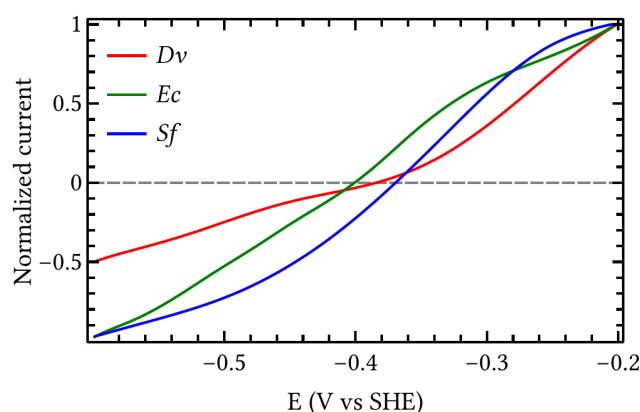


Figure 4: cyclic voltammograms obtained with the FDHs from *Dv* (100 mM CO<sub>2</sub>/NaHCO<sub>3</sub>, 50 mM KCl, 20 mM formate, 1 atm CO<sub>2</sub>, pH 6.5, 25 °C, data replotted from <sup>[65]</sup>), *Ec* (10 mM CO<sub>2</sub>, 10 mM formate, pH 6.8, 23 °C, data replotted from <sup>[63]</sup>), and *Sf* (10 mM CO<sub>2</sub>, 10 mM formate, pH 6.3, 37 °C, data replotted from <sup>[8]</sup>). The forward and backward scans were averaged in an attempt to remove most of the background current.

Walker and coworkers reported the only non-catalytic signals of FDH obtained so far with the FDH from *Cupriavidus necator* (formerly *Ralstonia eutropha*). By using a truncated form of the enzyme

and the possibility to produce an enzyme devoid of Mo, they could determine the reduction potential of the FeS cluster proximal to the Mo active site (at around -410 mV) and a 1-electron reduction potential attributed to the Mo VI/V transition (around -265 mV). The non-truncated form of this enzyme also shows catalytic oxidation of formate on the electrode, but CO<sub>2</sub> reduction was not observed.

Reversible catalytic voltammograms such as those of figure 4 cross the y=0 line at the Nernst potential of the CO<sub>2</sub>/HCOOH redox couple. Reda and Hirst took advantage of this feature to determine the CO<sub>2</sub>/HCOOH reduction potential between pH 4 and 7, and helped resolve a controversy about the actual value of the standard potential of the CO<sub>2</sub>/HCOOH couple<sup>[8]</sup>.

## Reductive activation

Reductive activations are commonly observed in the enzymes of the Mo/W bis-PGD family, like DMSO reductases<sup>[67]</sup>, periplasmic nitrate reductases<sup>[68,69]</sup>, and respiratory nitrate reductases<sup>[70,71]</sup>. It was also reported that several formate dehydrogenases activate upon reduction. In the case of *Dv* FdhAB, it is not possible to form an active film without a preliminary reductive activation in the presence of DTT<sup>[65]</sup>, or DTT and dithionite<sup>[57]</sup>. In the case of *Ec* FdhF, Robinson and coworkers could observe an activation process in voltammograms, in which the formate oxidation current was only present after a scan at low potentials<sup>[72]</sup>. A reduction step is also required for the Mo-FDH from *D. vulgaris* to become active in solution assays<sup>[61]</sup>.

The chemical nature of the activation process is yet unknown. Robinson and coworkers, on the basis of voltammograms of *Ec* FdhF, argued that the reductive activation is the decoordination of the SeCys from the active site metallic ion, to leave a free coordination site to which formate could bind<sup>[72]</sup>. However, this interpretation seems to contradict the more recent results of Oliveira and coworkers, who could resolve the crystal structure of the reduced enzyme, in which the SeCys is unambiguously coordinated to the W ion<sup>[54]</sup>. Perhaps the activation process is similar to the reductive activation in NapAB, the periplasmic nitrate reductase, for which it was proposed that the activation corresponds to a chemical modification of one of the molybdopterin ligands, possibly a ring closure/reduction<sup>[69]</sup>; detailed kinetic studies may help understanding the process in the future<sup>[73]</sup>.

## Kinetic studies

Robinson and coworkers used electrochemistry to study the response of *Ec* FdhF to a number of inhibitors, namely N<sub>3</sub><sup>-</sup>, OCN<sup>-</sup>, SCN<sup>-</sup>, NO<sub>3</sub><sup>-</sup> and NO<sub>2</sub><sup>-</sup><sup>[72]</sup>. They used chronoamperometry to systematically measure the fraction of inhibited enzymes for a range of inhibitor concentration, at different potentials and for different substrate concentrations, in both directions (formate oxidation and CO<sub>2</sub> reduction). They used a global fit approach to reproduce all their experimental data simultaneously, using a model allowing the binding of the inhibitors on any of the redox states of the active site: Mo(IV), Mo(V) and Mo(VI). The modeling yielded values of potentials for the redox couples of the active site, and the inhibition constants for each redox state. They found values of -365 mV for Mo(VI)/Mo(V), which is about 100 mV lower than what Walker and coworkers attributed to the Mo(VI)/Mo(V) transition in *Cupriavidus necator* FDH<sup>[64]</sup>, and -656 mV for Mo(V)/Mo(IV). All the inhibitors only coordinated significantly to the Mo(VI) state (with affinities of about 2 μM for N<sub>3</sub><sup>-</sup> and in the 50 to 100 μM range for the others), with the notable exception of NO<sub>2</sub><sup>-</sup>, which has very high affinity (sub micromolar) for Mo(V) and Mo(IV)<sup>[72]</sup>.

In a second step, Robinson and coworkers extended their modeling in another work, in which they did not use inhibitors but focused on the oxidation of formate, using a combination of stopped-flow kinetics, traditional solution assays and electrochemistry, also performing experiments with D-labeled formate. They used a global fitting approach to reproduce their data; they concluded that the formate binding steps and its “chemical processing” are strongly coupled<sup>[74]</sup>.

## Use of CO<sub>2</sub>-reducing enzymes in biotechnological applications

The use of CO<sub>2</sub>-reducing enzymes in biotechnological devices predates their study using electrochemistry. In the last few decades, CO<sub>2</sub>-reducing enzymes have been studied to find potential applications for CO<sub>2</sub> capture or to provide valuable carbon-based compounds which are only available from fossil fuels<sup>[6,75–79]</sup>. CODHs and FDHs have been used in different kinds of devices: coupled with photosensitizers to catalyze the photoreduction of CO<sub>2</sub>; coupled with a hydrogenase to catalyze the interconversion between formate and hydrogen or the water-gas shift reaction; or simply incorporated into electrodes for catalyzing the reduction of CO<sub>2</sub> or the oxidation of CO or formate.

### Photoreduction of CO<sub>2</sub>

One of the main objectives of the research on CO<sub>2</sub> reduction is artificial photosynthesis, with the goal of reproducing natural photosynthesis by using only light as energy source and water as source of electrons to reduce CO<sub>2</sub>. As neither CODH nor FDH are photosensitive (or even part of a photosynthetic carbon assimilation pathway<sup>[2]</sup>), this can only be achieved by using other components able to catalyse photoinduced charge separation, like natural photosystems, semi-conducting electrodes or synthetic photosensitizers.

The first example of photoelectrochemical CO<sub>2</sub> reduction catalyzed by an enzyme dates back to 1984, when Parkinson and Weaver combined a semiconductor photoelectrode (p-type indium phosphide) with the FDH from *Pseudomonas oxalaticus* (most probably a Mo-containing formate dehydrogenase<sup>[48,80]</sup>) to catalyze the two-electron reduction of CO<sub>2</sub> to formic acid<sup>[81]</sup>. This system employed methyl viologen (MV) as a redox mediator, and produced faradaic efficiencies between 80-93 % for the synthesis of formate.

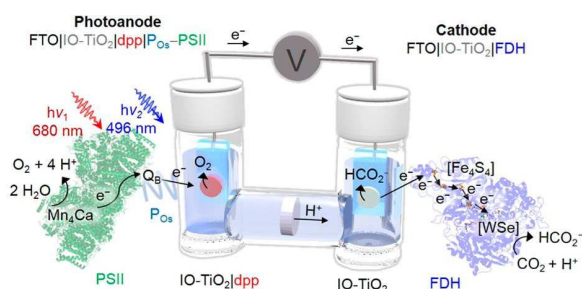


Figure 5 schematic view of the tandem cell used by Sokol and coworkers<sup>[82]</sup> to catalyze the photooxidation of water to O<sub>2</sub> at an anode incorporating photosystem II from *Thermosynechococcus elongatus* (left) coupled to the reduction of CO<sub>2</sub> to formate at a cathode

based on *D. vulgaris* FdhAB (right). Figure reproduced from <sup>[82]</sup> (Copyright © 2018 ACS, used with permission).

Perhaps the most emblematic work to date on the photoreduction of CO<sub>2</sub> is that from Sokol and coworkers, who coupled a previously developed<sup>[83]</sup> dye-photosensitized photosystem II-based photoanode capable of catalyzing the oxidation of water to O<sub>2</sub> to a hierarchically structured inverse opal TiO<sub>2</sub> cathode functionalized with *Dv* FdhAB (figure 5). This system performs the light-driven CO<sub>2</sub> conversion to formate using water as an electron donor, with a faradaic efficiency close to 80 %<sup>[82]</sup>. The FDH-functionalized cathode exhibited a good stability, retaining approximately 83 % of the initial activity after 2 h. The same team reported the coupling of *Dv* FdhAB to mesoporous metal-oxide electrodes (ITO and TiO<sub>2</sub>) for the electrocatalytic CO<sub>2</sub> reduction, and to dye-sensitized TiO<sub>2</sub> for the visible-light-driven CO<sub>2</sub> reduction<sup>[65]</sup>. In this other work, they used either ruthenium tris-2,2'-bipyridine complex (RuP) or diketopyrrolopyrrole (DPP) as photosensitizers to inject electrons into the conduction band of TiO<sub>2</sub> and drive the catalytic CO<sub>2</sub> reduction. The system achieved stable formate production for about 6 h, and approximately 36 % FDH remained active after 24 h of continuous photocatalysis.

Kuk and coworkers coupled the FDH from *Clostridium carboxydovorans* with an aldehyde dehydrogenase and an alcohol dehydrogenase in a tandem photoelectrochemical cell using a hematite-based photoanode and a bismuth ferrite-based photocathode. The photoelectrodes catalyzed photoreduction of NAD<sup>+</sup> to NADH coupled to the oxidation of water. When used with the three enzymes, and applying an external voltage of 0.8 V, the authors were able to photogenerate methanol, with a 32 % faradaic efficiency<sup>[84]</sup>.

CODHs were also used in photoelectrochemical devices for the reduction of CO<sub>2</sub> in several articles by Woolerton and coworkers. In a first example, the authors immobilized *Carboxydotherrmus hydrogenoformans* CODH I to TiO<sub>2</sub> nanoparticles functionalized with a Ru-bipyridine complex to catalyze the photoreduction of CO<sub>2</sub> to CO<sup>[85,86]</sup>. The system showed a turnover rate for the CODH of ~530 h<sup>-1</sup>, however the CO production rate fell to 25 % of its initial value after 4 h. Among several factors that were tested, the overall activity of the system improved only by increasing the amount of the anatase/rutile TiO<sub>2</sub> (P25) nanoparticles from 1 to 5 mg, and by using EDTA as the sacrificial electron donor to regenerate the photosensitizer. A second work reported on a similar device with the same *Ch* CODH I, but this time immobilized on TiO<sub>2</sub> nanoparticles coated with silver nanoclusters stabilized by polymethacrylic acid (AgNCs-PMAA)<sup>[87]</sup>. The AgNCs-PMAA coating greatly enhanced the activity of the TiO<sub>2</sub>/CODH electrode for CO<sub>2</sub> photoreduction, which was stable over several hours and for at least 250 000 turnovers of the enzyme's active site (a turnover frequency of 20 s<sup>-1</sup> was determined under visible-light irradiation). The same group later demonstrated that connecting *Ch* CODH I to carefully chosen semi-conducting electrodes can significantly alter the bias, to the point of almost suppressing the oxidation of CO<sup>[88]</sup>. The authors argued that slowing down the oxidation of CO may be desirable in the context of artificial photosynthesis, where the purpose is to accumulate the reduction product and prevent back reactions<sup>[88]</sup>. This article did not actually feature photoreduction of CO<sub>2</sub>.

Amao and coworkers also reported on photochemical devices for the production of formate. In a first article, the authors investigated the metal-free FDH from *Saccharomyces cerevisiae* immobilized onto viologen-functionalized ITO electrodes for the light-driven production of formate<sup>[89]</sup>. The same strategy to co-immobilize FDH and viologen onto an optically transparent conductive glass electrode (tin oxide) was used to construct the cathode of a visible-light photo-biofuel cell working with CO<sub>2</sub> and glucose<sup>[90]</sup>. The biocatalyst of the anode was glucose dehydrogenase with NAD<sup>+</sup>, and the open-circuit photovoltage of the cell was 390 mV, with an

estimated maximum power of  $57 \mu\text{W cm}^{-2}$ . More recently, the same group designed a new visible light-driven biofuel cell with the same type of FDH/viologen cathode (employing the metal-free FDH from *Candida boidinii*) and a nanocrystalline  $\text{TiO}_2$  photoanode covered with the thylakoid membrane of microalgae *Spirulina platensis* (containing photosystems I and II, and redox proteins)<sup>[91]</sup>. Using a  $\text{CO}_2$ -saturated buffer solution as electrolyte, the solar cell produced formate and oxygen stoichiometrically while generating electricity.

## Coupling $\text{CO}_2$ reduction with the oxidation of $\text{H}_2$ or other electron sources

Except for the solar cells described above, there is only one example in the literature of a  $\text{CO}_2$ -reducing fully enzymatic fuel cell, capable of generating formate without any external power supply. Such a biofuel cell was constituted of a biocathode with W-containing FDH from *M. extorquens* co-adsorbed on a gas-diffusion electrode with benzyl viologen as the redox mediator, and a bioanode with the NiFe hydrogenase from *D. vulgaris* Miyazaki adsorbed on a second gas-diffusion electrode functionalized with p-phenylenediamine in order to perform  $\text{H}_2$  oxidation under conditions of direct electron transfer<sup>[92]</sup>. The gas-diffusion system allowed the supply of both gaseous substrates ( $\text{H}_2$  and  $\text{CO}_2$ ) at high rates, however the faradaic efficiency for formate production was relatively low (around 20 %), which was attributed to the competing reduction of  $\text{O}_2$  present in the gas supply at the  $\text{CO}_2$ -reducing cathode.

Another example of a system coupling FDH and hydrogenase is the semi-artificial formate hydrogenlyase (FHL) complex reported by Sokol and coworkers<sup>[93]</sup>. This complex, naturally present in *E. coli*, couples in vivo the oxidation of formate to the production of  $\text{H}_2$  under conditions of fermentative growth<sup>[94,95]</sup>. In an effort to mimic the functionality of the FHL complex, the FDH and NiFe hydrogenase from *D. vulgaris* Hildenborough were wired to macro-mesoporous inverse opal ITO electrodes, retaining a good activity for 24 h, with faradaic efficiencies for formate and  $\text{H}_2$  production of 76 and 77 %, respectively.



Figure 6: schematic representation of the graphite platelets used by Lazarus and coworkers to catalyze the water-gas shift reaction. CO is oxidized to  $\text{CO}_2$  by the CODH on the left, and the electrons generated are transferred via the graphite to the hydrogenase on the right, which produces  $\text{H}_2$ . Figure reproduced from <sup>[96]</sup> (Copyright © 2009 ACS, used with permission).

CODHs were also coupled with hydrogenases in order to catalyze the water-gas shift (WGS) reaction, an industrially important process for converting CO into  $\text{H}_2$ :



This reaction requires high temperatures catalysis in current industrial processes (in excess of 500 K). Lazarus and coworkers reported a system in which two NiFe enzymes (*Ch* CODH I and the hydrogenase Hyd-2 from *E. coli*) were co-immobilized on a conducting graphite platelet, which acts as an electron mediator between the enzymes (figure 6). Despite a moderate driving force for

the WGS reaction, this catalytic system showed high rates at low temperatures, comparable to those of synthetic catalysts at high temperatures<sup>[96]</sup>. The simultaneous H<sub>2</sub> production / CO consumption was shown to continuously occur in an experiment lasting over 55 h, and the system was stable for at least 14 days when stored anaerobically at 4 °C.

Another example of a multi-enzymatic system catalyzing the reduction of CO<sub>2</sub> is the heterodisulfide reductase supercomplex from the methanogenic archaeon *Methanococcus maripaludis*, which was adsorbed to graphite electrodes. This complex is composed of a heterodisulfide reductase, a formate dehydrogenase, and a NiFe hydrogenase. It was immobilized by adsorption onto graphite bar electrodes, and was shown to continuously catalyze the reduction of CO<sub>2</sub> to formate with a faradaic efficiency around 90 % for extended periods of time (6 days) with moderate loss of activity<sup>[97]</sup>. In this study, the purification of the FDH from the complex was not required for the reduction of CO<sub>2</sub>, which simplifies the electrode preparation procedure.

The FDH from *Methanococcus maripaludis* was also employed in another system that coupled the oxidation of dilute organic compounds (like in wastewater) in a microbial battery to the enzymatic reduction of CO<sub>2</sub> or protons<sup>[98]</sup>. The originality of that work was to use solid-state electrodes based on prussian blue both as cathodes for the microbial battery and as anodes for the enzymatic generation of reduced compounds, swapping them to regenerate them. The driving force for the enzymatic reduction is provided by the electromotive force generated by the microbial battery.

## Electrodes for CO<sub>2</sub> reduction

In the last section of this part, we focus on studies connecting or improving the connection of CO<sub>2</sub>-reducing enzymes to electrodes. Two strategies are employed for wiring the enzymes to electrodes: using mediators, redox moieties that can shuttle electrons between the electrode and the redox enzyme, or immobilizing the enzymes on the electrode in a configuration where the electron transfer is direct.

### Mediated electron transfer

In the case of mediated electron transfer (MET), the match between the potential of the mediator and that of the reaction is an important factor for the efficiency of the intermolecular electron transfer. However, as was recently shown by the observation of reversible catalysis in the case of mediated electron transfer<sup>[99]</sup>, and contrary to what is commonly accepted, a favorable driving force for the electron transfer is not strictly required, because the requirements for efficient electron mediation are purely kinetic: the electrons only have to be transferred fast enough in the direction of the catalysis<sup>[99]</sup>. This requirement naturally prevents the use of mediators whose potentials are too far off, unless they exchange electrons with the enzyme at an exceptionally high rate.

The mediators used for CO<sub>2</sub>-reducing enzymes have either been used directly in solution or attached to side chains of polymer to form redox hydrogels. The most widely used redox mediators are viologen derivatives, such as methyl viologen (MV, with  $E^{0'} = -0.45$  V vs. SHE) and benzyl viologen (BV, with  $E^{0'} = -0.37$  V vs. SHE)<sup>[100]</sup>. In particular, MV has been employed in many studies as a mediator for CO<sub>2</sub> electroreduction catalyzed by FDH<sup>[81,89-91]</sup> and CODH<sup>[101]</sup>, since its reduction potential (independent of pH) is comparable to that of the CO<sub>2</sub>/HCOO<sup>-</sup> couple ( $E^{0'} = -0.43$  V vs. SHE at pH 7<sup>[102]</sup>), and hardly higher than that of the CO<sub>2</sub>/CO couple ( $E^{0'} = -0.53$  V vs. SHE at pH 7).

Shin and coworkers were the first to report mediated electrochemistry of a CODH, the ACS/CODH from *Moorella thermoacetica*. They used MV and a glassy carbon electrode to catalyze the reduction of CO<sub>2</sub> to CO at -0.57 V vs. SHE, with a faradaic efficiency close to 100 %<sup>[101]</sup>.

Sakai and coworkers published a comprehensive study including several redox mediators suitable for CO<sub>2</sub> reduction and formate oxidation catalyzed by FDH<sup>[103]</sup>. The authors studied the mediated electrochemistry in solution of the W-containing formate dehydrogenase from *Methylobacterium extorquens* with 12 different mediators for formate oxidation (including its natural electron acceptor NAD<sup>+</sup>) and 3 different mediators for CO<sub>2</sub> reduction. They concluded that the best mediator for formate oxidation was 9,10-phenanthrenequinone, and the best one for CO<sub>2</sub> reduction was MV. The latter was in fact used both for formate oxidation and for the reduction of CO<sub>2</sub> in the same system but at different pHs<sup>[104]</sup>. In another study, they reported the construction of a gas-diffusion biocathode for CO<sub>2</sub> reduction using the same enzyme as catalyst, with freely diffusing 1,1'-trimethylene-2,2'-bipyridinium dibromide (TQ) as electron mediator<sup>[105]</sup>. TQ ( $E^{0'}$  = -0.54 V vs. SHE) has a lower reduction potential than MV and is better suited for CO<sub>2</sub> reduction to formate at pH 7.

Although this is not strictly speaking an electrochemical device, Reginald and coworkers very recently demonstrated a CO sensor based on the MoCu CODH. The principle of the device is to use CODH to oxidize CO to CO<sub>2</sub>, employing methylene blue as a sacrificial electron acceptor, and rely on a newly designed CO<sub>2</sub> sensor to detect the product of the reaction<sup>[106]</sup>.

## Direct electron transfer

Alvarez-Malmagro and coworkers also recently showed efficient CO<sub>2</sub> electroreduction by using Dv FdhAB covalently immobilized on low-density graphite (LDG) electrodes, with MV as a mediator<sup>[107]</sup>. Interestingly, the enzyme worked also in direct electron transfer (DET) since the electrodes were modified with amino groups, suitable for the covalent attachment of FDH with an orientation favorable for DET (most exposed [4Fe4S] cluster facing the electrode surface). Formate oxidation was also shown, with current densities higher than those of CO<sub>2</sub> reduction, both for DET and MET (with BV as a mediator in the latter case), with the enzyme immobilized on either gold or LDG electrodes.

The immobilization of CODH on electrodes under conditions of direct electron transfer was also optimized, with the recent report of the immobilization of a recombinant CODH from *Rhodospirillum rubrum* on multiwalled carbon nanotube (MWCNT) electrodes modified with 1-pyrenebutyric acid adamantyl amide, a promoter that favors immobilization of metalloenzymes on carbon nanotubes<sup>[34]</sup>. The authors could obtain current densities of 0.35 mA cm<sup>-2</sup> at -0.3 V vs. SHE for the oxidation of CO and 2.9 mA cm<sup>-2</sup> at -0.75 V vs. SHE for the reduction of CO<sub>2</sub>. When the CODH/MWCNT film was used on a gas-diffusion electrode, thus circumventing gas substrate solubility and diffusion issues, the current density reached values of 1.5 mA cm<sup>-2</sup> at -0.38 V for CO oxidation, and 4.2 mA cm<sup>-2</sup> at -0.8 V for CO<sub>2</sub> reduction. The greater increase in current for the CO oxidation is presumably due to the fact that the diffusion of CO in solution is more rate limiting than the diffusion of CO<sub>2</sub>, in line with the far greater solubility of CO<sub>2</sub> in water.

## Incorporation into redox hydrogels

The incorporation of redox enzymes into redox hydrogels has raised significant interest over the past decades. The benefits are numerous, since the incorporation increases the loading of enzyme on the electrode, ensures electrical connection as in a standard mediated electrochemistry in solution, while preventing enzyme leaching to the electrolyte<sup>[108–110]</sup>. This approach has gained in generality when it was demonstrated that they can protect O<sub>2</sub>-sensitive enzymes like hydrogenases against inactivation by O<sub>2</sub>, under oxidation catalysis<sup>[111–113]</sup>; the use of redox hydrogels for reductive catalysis is also steadily developing<sup>[99,114]</sup>.

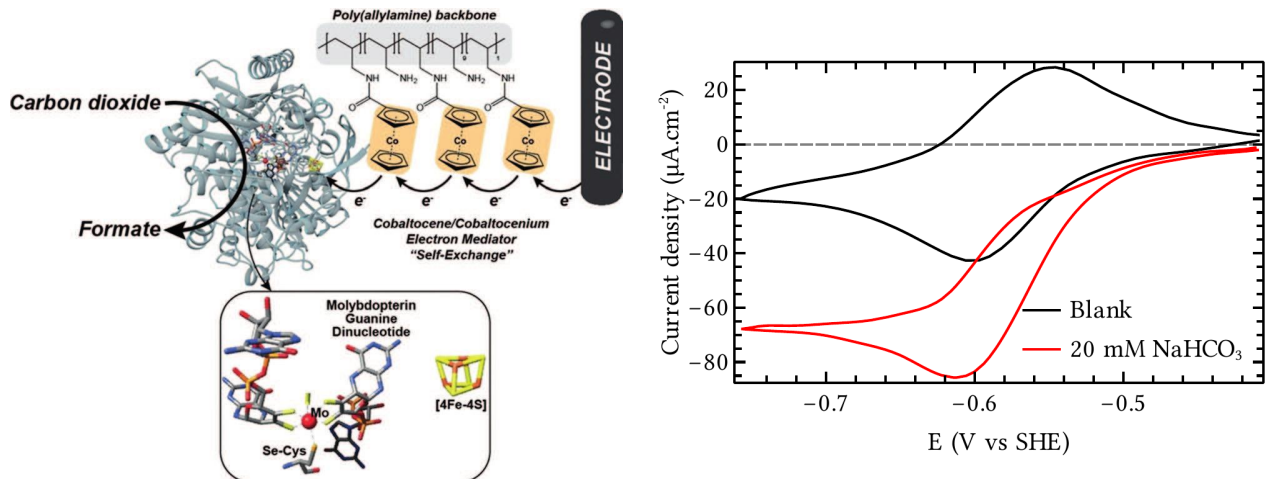


Figure 7: cobaltocene-based redox film incorporating *E. coli* FDH for the reduction of CO<sub>2</sub>. Left: scheme of the device, showing the electron transfer from the electrode to the FDH mediated by hopping across the immobilized cobaltocene moieties. Right: cyclic voltammograms showing the reduction of CO<sub>2</sub>. Data reproduced from <sup>[115]</sup> with permission.

Yuan and coworkers recently demonstrated the successful inclusion of *Ec* FDH into a low-potential cobaltocene (Cc)-based redox hydrogel for the production of formate<sup>[115]</sup> (figure 7). The reduction potential of the polymer (a Cc-functionalized poly(allylamine)) was determined at -0.576 V vs. SHE, way more negative than that of the couple CO<sub>2</sub>/HCOO<sup>-</sup>, being the refore suitable to mediate electron transfer for CO<sub>2</sub> reduction catalyzed by the Mo-FDH. Bulk electrolysis analysis determined a faradaic efficiency of 99 % for formate production, and the bioelectrode retained about 65 % of its initial activity after 12 h of continuous operation. Another conductive polymer widely used with redox enzymes is the polyaniline (PANi) hydrogel, which has been employed also to immobilize the W-containing FDH from *Clostridium ljungdahlii* onto a bioelectrode for CO<sub>2</sub> reduction<sup>[116]</sup>. This system could also successfully convert CO<sub>2</sub> to formate during 12 h of reaction, with a faradaic efficiency of about 93 %. Finally, in a very recent example, the above-mentioned *D. vulgaris* Hildenborough FDH was immobilized on carbon cloth using a viologen-functionalized polymer (with E<sup>0</sup> = -0.39 V vs. SHE) to construct a CO<sub>2</sub>-reducing gas-diffusion biocathode<sup>[117]</sup>. By modifying the microporous side of the carbon cloth with the polymer/FDH film, the electrode showed high non-catalytic and catalytic currents, with a stable current output for CO<sub>2</sub> reduction over 45 h, preserving approximately 80 % of its initial activity.

## Summary and outlook

CO dehydrogenases and formate dehydrogenases are the only enzymes that directly reduce CO<sub>2</sub>, hence their interest either as source of inspiration, or as catalyst in biotechnological devices. The number of works in which either of this enzyme was connected to electrodes have grown steadily since the first studies in the mid-2000. These studies have brought significant breakthroughs, like the development of highly efficient systems for the reduction of CO<sub>2</sub>, and significant advances in the understanding of the catalytic mechanisms of both CODH and FDH. It is our opinion that this is only the beginning, and that the forthcoming years will bring their share of high quality studies of the catalytic mechanism of FDH or CODH using electrochemistry, and original and more efficient devices for the reduction of CO<sub>2</sub>.

## Acknowledgements

The authors acknowledge support from CNRS, Aix-Marseille Université, Agence Nationale de la Recherche (ANR-15-CE05-0020, ANR-16-CE29-0010-01, ANR-17-CE11-002), and the Excellence Initiative of Aix-Marseille University - A\*MIDEX, a French “Investissements d’Avenir” programme (ANR-11-IDEX-0001-02), and the ANR-DFG project SHIELDS (PL 746/2-1). They are part of FrenchBIC (<http://frenchbic.cnrs.fr>).

## References

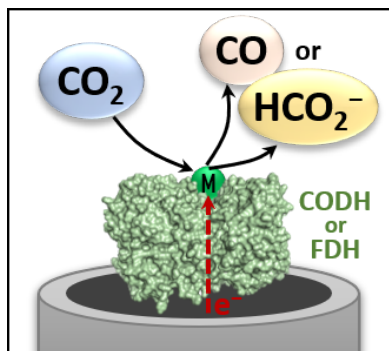
- [1] V. Fourmond, *Anal. Chem.* **2016**, *88*, 5050–5052.
- [2] A. Bar-Even, E. Noor, R. Milo, *J. Exp. Bot.* **2012**, *63*, 2325–2342.
- [3] G. Fuchs, *Annu. Rev. Microbiol.* **2011**, *65*, 631–658.
- [4] I. Andersson, A. Backlund, *Plant Physiol. Biochem.* **2008**, *46*, 275–291.
- [5] S. W. Ragsdale, *Chem. Rev.* **2003**, *103*, 2333–2346.
- [6] A. M. Appel, J. E. Bercaw, A. B. Bocarsly, H. Dobbek, D. L. DuBois, M. Dupuis, J. G. Ferry, E. Fujita, R. Hille, P. J. A. Kenis, C. A. Kerfeld, R. H. Morris, C. H. F. Peden, A. R. Portis, S. W. Ragsdale, T. B. Rauchfuss, J. N. H. Reek, L. C. Seefeldt, R. K. Thauer, G. L. Waldrop, *Chem. Rev.* **2013**, *113*, 6621–6658.
- [7] S. W. Ragsdale, E. Pierce, *Biochim. Biophys. Acta* **2008**, *1784*, 1873–1898.
- [8] T. Reda, C. M. Plugge, N. J. Abram, J. Hirst, *Proc. Natl. Acad. Sci. U. S. A.* **2008**, *105*, 10654–10658.
- [9] A. Parkin, J. Seravalli, K. A. Vincent, S. W. Ragsdale, F. A. Armstrong, *J. Am. Chem. Soc.* **2007**, *129*, 10328–10329.
- [10] V. Fourmond, N. Plumeré, C. Léger, *Nat. Rev. Chem.* **2021**, *5*, 348–360.
- [11] V. Svetlitchnyi, C. Peschel, G. Acker, O. Meyer, *J. Bacteriol.* **2001**, *183*, 5134–5144.
- [12] C. Léger, P. Bertrand, *Chem. Rev.* **2008**, *108*, 2379–2438.
- [13] M. del Barrio, M. Sensi, C. Orain, C. Baffert, S. Dementin, V. Fourmond, C. Léger, *Acc. Chem. Res.* **2018**, *51*, 769–777.
- [14] J. Hirst, *Biochim. Biophys. Acta* **2006**, *1757*, 225–239.
- [15] F. A. Armstrong, N. A. Belsey, J. A. Cracknell, G. Goldet, A. Parkin, E. Reisner, K. A. Vincent, A. F. Wait, *Chem. Soc. Rev.* **2009**, *38*, 36–51.
- [16] P. Kaufmann, B. R. Duffus, C. Teutloff, S. Leimkühler, *Biochemistry* **2018**, *57*, 2889–2901.
- [17] R. Hille, S. Dingwall, J. Wilcoxon, *J. Biol. Inorg. Chem.* **2015**, *20*, 243–251.
- [18] M. Can, F. A. Armstrong, S. W. Ragsdale, *Chem. Rev.* **2014**, *114*, 4149–4174.
- [19] H. Dobbek, V. Svetlitchnyi, L. Gremer, R. Huber, O. Meyer, *Science* **2001**, *293*, 1281–1285.
- [20] C. L. Drennan, J. Heo, M. D. Sintchak, E. Schreiter, P. W. Ludden, *Proc. Natl. Acad. Sci. U. S. A.* **2001**, *98*, 11973–11978.
- [21] E. C. Wittenborn, M. Merrouch, C. Ueda, L. Fradale, C. Léger, V. Fourmond, M.-E. Pandelia, S. Dementin, C. L. Drennan, *Elife* **2018**, *7*, DOI 10.7554/eLife.39451.

- [22] C. Darnault, A. Volbeda, E. J. Kim, P. Legrand, X. Vernède, P. A. Lindahl, J. C. Fontecilla-Camps, *Nat. Struct. Biol.* **2003**, *10*, 271–279.
- [23] M. Inoue, I. Nakamoto, K. Omae, T. Oguro, H. Ogata, T. Yoshida, Y. Sako, *Front. Microbiol.* **2018**, *9*, 3353.
- [24] M. Wu, Q. Ren, A. S. Durkin, S. C. Daugherty, L. M. Brinkac, R. J. Dodson, R. Madupu, S. A. Sullivan, J. F. Kolonay, D. H. Haft, W. C. Nelson, L. J. Tallon, K. M. Jones, L. E. Ulrich, J. M. Gonzalez, I. B. Zhulin, F. T. Robb, J. A. Eisen, *PLoS Genet.* **2005**, *1*, e65.
- [25] M. C. Schoelmerich, V. Müller, *Proc. Natl. Acad. Sci. U. S. A.* **2019**, *116*, 6329–6334.
- [26] L. Domnik, M. Merrouch, S. Goetzl, J.-H. Jeoung, C. Léger, S. Dementin, V. Fourmond, H. Dobbek, *Angew. Chem. Int. Ed Engl.* **2017**, *56*, 15466–15469. *Angew. Chem.* **2017**, *129*, 15670–15674.
- [27] L. Rajeev, K. L. Hillesland, G. M. Zane, A. Zhou, M. P. Joachimiak, Z. He, J. Zhou, A. P. Arkin, J. D. Wall, D. A. Stahl, *J. Bacteriol.* **2012**, *194*, 5783–5793.
- [28] M. Merrouch, Mécanisme, Maturation et Biodiversité D'une Enzyme à Cofacteur NiFe, Importante Dans Le Contexte de L'énergie et de L'environnement : La Carbone Monoxyde Déshydrogénase, Aix-Marseille Université, **2017**.
- [29] J.-H. Jeoung, H. Dobbek, *Science* **2007**, *318*, 1461–1464.
- [30] H. Dobbek, V. Svetlitchnyi, J. Liss, O. Meyer, *J. Am. Chem. Soc.* **2004**, *126*, 5382–5387.
- [31] M. Kumar, W. P. Lu, L. Liu, S. W. Ragsdale, *J. Am. Chem. Soc.* **1993**, *115*, 11646–11647.
- [32] P. Amara, J.-M. Mousca, A. Volbeda, J. C. Fontecilla-Camps, *Inorg. Chem.* **2011**, *50*, 1868–1878.
- [33] R. Breglia, F. Arrigoni, M. Sensi, C. Greco, P. Fantucci, L. De Gioia, M. Bruschi, *Inorg. Chem.* **2021**, *60*, 387–402.
- [34] U. Contaldo, B. Guigliarelli, J. Perard, C. Rinaldi, A. Le Goff, C. Cavazza, *ACS Catalysis* **2021**, *11*, 5808–5817.
- [35] C. Léger, S. Dementin, P. Bertrand, M. Rousset, B. Guigliarelli, *J. Am. Chem. Soc.* **2004**, *126*, 12162–12172.
- [36] M. Benvenuti, M. Meneghello, C. Guendon, A. Jacq-Bailly, J.-H. Jeoung, H. Dobbek, C. Léger, V. Fourmond, S. Dementin, *Biochim. Biophys. Acta Bioenerg.* **2020**, *1861*, 148188.
- [37] V. C.-C. Wang, S. W. Ragsdale, F. A. Armstrong, *Chembiochem* **2013**, *14*, 1845–1851.
- [38] M. Merrouch, J. Hadj-Saïd, C. Léger, S. Dementin, V. Fourmond, *Electrochim. Acta* **2017**, *245*, 1059–1064.
- [39] A. Bar-Even, E. Noor, Y. Savir, W. Liebermeister, D. Davidi, D. S. Tawfik, R. Milo, *Biochemistry* **2011**, *50*, 4402–4410.
- [40] V. C.-C. Wang, M. Can, E. Pierce, S. W. Ragsdale, F. A. Armstrong, *J. Am. Chem. Soc.* **2013**, *135*, 2198–2206.
- [41] V. C.-C. Wang, S. T. A. Islam, M. Can, S. W. Ragsdale, F. A. Armstrong, *J. Phys. Chem. B* **2015**, *119*, 13690–13697.
- [42] M. Merrouch, J. Hadj-Saïd, L. Domnik, H. Dobbek, C. Léger, S. Dementin, V. Fourmond, *Chemistry* **2015**, *21*, 18934–18938.
- [43] E. C. Wittenborn, C. Guendon, M. Merrouch, M. Benvenuti, V. Fourmond, C. Léger, C. L. Drennan, S. Dementin, *ACS Catal.* **2020**, *10*, 7328–7335.
- [44] J. Hadj-Saïd, La CO déshydrogénase de *Desulfovibrio vulgaris*, Aix Marseille Université, **2015**.
- [45] A. K. Jones, S. E. Lamle, H. R. Pershad, K. A. Vincent, S. P. J. Albracht, F. A. Armstrong, *J. Am. Chem. Soc.* **2003**, *125*, 8505–8514.
- [46] V. Fourmond, P. Infossi, M.-T. Giudici-Ortoni, P. Bertrand, C. Léger, *J. Am. Chem. Soc.* **2010**, *132*, 4848–4857.
- [47] V. I. Tishkov, V. O. Popov, *Biochemistry* **2004**, *69*, 1252–1267.
- [48] R. Hille, J. Hall, P. Basu, *Chem. Rev.* **2014**, *114*, 3963–4038.
- [49] S. Grimaldi, B. Schoepp-Cothenet, P. Ceccaldi, B. Guigliarelli, A. Magalon, *Biochim. Biophys. Acta* **2013**, *1827*, 1048–1085.
- [50] S. Leimkühler, C. Iobbi-Nivol, *FEMS Microbiol. Rev.* **2016**, *40*, 1–18.
- [51] R. Thomé, A. Gust, R. Toci, R. Mendel, F. Bittner, A. Magalon, A. Walburger, *J. Biol. Chem.* **2012**, *287*, 4671–4678.
- [52] P. Arnoux, C. Ruppelt, F. Oudouhou, J. Lavergne, M. I. Siponen, R. Toci, R. R. Mendel, F. Bittner, D. Pignol, A. Magalon, A. Walburger, *Nat. Commun.* **2015**, *6*, 6148.

- [53] J. C. Boyington, V. N. Gladyshev, S. V. Khangulov, T. C. Stadtman, P. D. Sun, *Science* **1997**, *275*, 1305–1308.
- [54] A. R. Oliveira, C. Mota, C. Mourato, R. M. Domingos, M. F. A. Santos, D. Gesto, B. Guigliarelli, T. Santos-Silva, M. J. Romão, I. A. Cardoso Pereira, *ACS Catal.* **2020**, *10*, 3844–3856.
- [55] S. V. Khangulov, V. N. Gladyshev, G. C. Dismukes, T. C. Stadtman, *Biochemistry* **1998**, *37*, 3518–3528.
- [56] T. G. Cooper, T. T. Tchen, H. G. Wood, C. R. Benedict, *J. Biol. Chem.* **1968**, *243*, 3857–3863.
- [57] M. Meneghello, A. R. Oliveira, A. Jacq-Bailly, I. A. C. Pereira, C. Léger, V. Fourmond, *Angew. Chem. Int. Ed Engl.* **2021**, *60*, 9964–9967. *Angew. Chem.* **2021**, *133*, 10052–10055.
- [58] L. B. Maia, J. J. G. Moura, I. Moura, *J. Biol. Inorg. Chem.* **2015**, *20*, 287–309.
- [59] H. C. A. Raaijmakers, M. J. Romão, *J. Biol. Inorg. Chem.* **2006**, *11*, 849–854.
- [60] C. S. Mota, M. G. Rivas, C. D. Brondino, I. Moura, J. J. G. Moura, P. J. González, N. M. F. S. A. Cerqueira, *J. Biol. Inorg. Chem.* **2011**, *16*, 1255–1268.
- [61] L. B. Maia, L. Fonseca, I. Moura, J. J. G. Moura, *J. Am. Chem. Soc.* **2016**, *138*, 8834–8846.
- [62] D. Niks, J. Duvvuru, M. Escalona, R. Hille, *J. Biol. Chem.* **2016**, *291*, 1162–1174.
- [63] A. Bassegoda, C. Madden, D. W. Wakerley, E. Reisner, J. Hirst, *J. Am. Chem. Soc.* **2014**, *136*, 15473–15476.
- [64] L. M. Walker, B. Li, D. Niks, R. Hille, S. J. Elliott, *J. Biol. Inorg. Chem.* **2019**, *24*, 889–898.
- [65] M. Miller, W. E. Robinson, A. R. Oliveira, N. Heidary, N. Kornienko, J. Warnan, I. A. C. Pereira, E. Reisner, *Angew. Chem. Int. Ed Engl.* **2019**, *58*, 4601–4605. *Angew. Chem.* **2019**, *131*, 4649–4653.
- [66] A. Abou Hamdan, S. Dementin, P.-P. Liebgott, O. Gutierrez-Sanz, P. Richaud, A. L. De Lacey, M. Rousset, P. Bertrand, L. Cournac, C. Léger, *J. Am. Chem. Soc.* **2012**, *134*, 8368–8371.
- [67] R. C. Bray, B. Adams, A. T. Smith, B. Bennett, S. Bailey, *Biochemistry* **2000**, *39*, 11258–11269.
- [68] V. Fourmond, B. Burlat, S. Dementin, P. Arnoux, M. Sabaty, S. Boiry, B. Guigliarelli, P. Bertrand, D. Pignol, C. Léger, *J. Phys. Chem. B* **2008**, *112*, 15478–15486.
- [69] J. G. J. Jacques, V. Fourmond, P. Arnoux, M. Sabaty, E. Etienne, S. Grosse, F. Biaso, P. Bertrand, D. Pignol, C. Léger, B. Guigliarelli, B. Burlat, *Biochim. Biophys. Acta* **2014**, *1837*, 277–286.
- [70] S. J. Field, N. P. Thornton, L. J. Anderson, A. J. Gates, A. Reilly, B. J. N. Jepson, D. J. Richardson, S. J. George, M. R. Cheesman, J. N. Butt, *Dalton Trans.* **2005**, 3580–3586.
- [71] P. Ceccaldi, J. Rendon, C. Léger, R. Toci, B. Guigliarelli, A. Magalon, S. Grimaldi, V. Fourmond, *Biochim. Biophys. Acta* **2015**, *1847*, 1055–1063.
- [72] W. E. Robinson, A. Bassegoda, E. Reisner, J. Hirst, *J. Am. Chem. Soc.* **2017**, *139*, 9927–9936.
- [73] M. del Barrio, V. Fourmond, *ChemElectroChem* **2019**, *6*, 4949–4962.
- [74] W. E. Robinson, A. Bassegoda, J. N. Blaza, E. Reisner, J. Hirst, *J. Am. Chem. Soc.* **2020**, *142*, 12226–12236.
- [75] M. Beller, U. T. Bornscheuer, *Angew. Chem. Int. Ed Engl.* **2014**, *53*, 4527–4528. *Angew. Chem.* **2014**, *126*, 4615–4617.
- [76] C. Costentin, M. Robert, J.-M. Savéant, *Chem. Soc. Rev.* **2013**, *42*, 2423–2436.
- [77] E. E. Benson, C. P. Kubiak, A. J. Sathrum, J. M. Smieja, *Chem. Soc. Rev.* **2009**, *38*, 89–99.
- [78] J. Qiao, Y. Liu, F. Hong, J. Zhang, *Chem. Soc. Rev.* **2014**, *43*, 631–675.
- [79] T. W. Woolerton, S. Sheard, Y. S. Chaudhary, F. A. Armstrong, *Energy Environ. Sci.* **2012**, *5*, 7470.
- [80] U. Müller, P. Willnow, U. Ruschig, T. Höpner, *Eur. J. Biochem.* **1978**, *83*, 485–498.
- [81] B. A. Parkinson, P. F. Weaver, *Nature* **1984**, *309*, 148–149.
- [82] K. P. Sokol, W. E. Robinson, A. R. Oliveira, J. Warnan, M. M. Nowaczyk, A. Ruff, I. A. C. Pereira, E. Reisner, *J. Am. Chem. Soc.* **2018**, *140*, 16418–16422.
- [83] K. P. Sokol, W. E. Robinson, J. Warnan, N. Kornienko, M. M. Nowaczyk, A. Ruff, J. Z. Zhang, E. Reisner, *Nat. Energy* **2018**, *3*, 944–951.
- [84] S. K. Kuk, R. K. Singh, D. H. Nam, R. Singh, J.-K. Lee, C. B. Park, *Angew. Chem. Int. Ed Engl.* **2017**, *56*, 3827–3832. *Angew. Chem.* **2017**, *129*, 3885–3890.
- [85] T. W. Woolerton, S. Sheard, E. Reisner, E. Pierce, S. W. Ragsdale, F. A. Armstrong, *J. Am. Chem. Soc.* **2010**, *132*, 2132–2133.

- [86] T. W. Woolerton, S. Sheard, E. Pierce, S. W. Ragsdale, F. A. Armstrong, *Energy Environ. Sci.* **2011**, *4*, 2393.
- [87] L. Zhang, M. Can, S. W. Ragsdale, F. A. Armstrong, *ACS Catal.* **2018**, *8*, 2789–2795.
- [88] A. Bachmeier, V. C. C. Wang, T. W. Woolerton, S. Bell, J. C. Fontecilla-Camps, M. Can, S. W. Ragsdale, Y. S. Chaudhary, F. A. Armstrong, *J. Am. Chem. Soc.* **2013**, *135*, 15026–15032.
- [89] Y. Amao, N. Shuto, *Research on Chemical Intermediates* **2014**, *40*, 3267–3276.
- [90] Y. Amao, N. Shuto, *Journal of Porphyrins and Phthalocyanines* **2015**, *19*, 459–464.
- [91] Y. Amao, M. Fujimura, M. Miyazaki, A. Tadokoro, M. Nakamura, N. Shuto, *New Journal of Chemistry* **2018**, *42*, 9269–9280.
- [92] T. Adachi, Y. Kitazumi, O. Shirai, K. Kano, *Electrochemistry Communications* **2018**, *97*, 73–76.
- [93] K. P. Sokol, W. E. Robinson, A. R. Oliveira, S. Zacarias, C.-Y. Lee, C. Madden, A. Bassegoda, J. Hirst, I. A. C. Pereira, E. Reisner, *J. Am. Chem. Soc.* **2019**, *141*, 17498–17502.
- [94] J. S. McDowall, B. J. Murphy, M. Haumann, T. Palmer, F. A. Armstrong, F. Sargent, *Proc. Natl. Acad. Sci. U. S. A.* **2014**, *111*, E3948–56.
- [95] J. S. McDowall, M. C. Hjersing, T. Palmer, F. Sargent, *FEBS Lett.* **2015**, *589*, 3141–3147.
- [96] O. Lazarus, T. W. Woolerton, A. Parkin, M. J. Lukey, E. Reisner, J. Seravalli, E. Pierce, S. W. Ragsdale, F. Sargent, F. A. Armstrong, *J. Am. Chem. Soc.* **2009**, *131*, 14154–14155.
- [97] M. Lienemann, J. S. Deutzmann, R. D. Milton, M. Sahin, A. M. Spormann, *Bioresour. Technol.* **2018**, *254*, 278–283.
- [98] K. L. Dubrawski, X. Shao, R. D. Milton, J. S. Deutzmann, A. M. Spormann, C. S. Criddle, *ACS Energy Lett.* **2019**, *4*, 2929–2936.
- [99] S. Hardt, S. Stapf, D. T. Filmon, J. A. Birrell, O. Rüdiger, V. Fourmond, C. Léger, N. Plumeré, *Nat Catal* **2021**, *4*, 251–258.
- [100] P. Wardman, *Free Radic. Res. Commun.* **1991**, *14*, 57–67.
- [101] W. Shin, S. H. Lee, J. W. Shin, S. P. Lee, Y. Kim, *J. Am. Chem. Soc.* **2003**, *125*, 14688–14689.
- [102] W. Zhang, Y. Hu, L. Ma, G. Zhu, Y. Wang, X. Xue, R. Chen, S. Yang, Z. Jin, *Advanced Science* **2018**, *5*, 1700275.
- [103] K. Sakai, B.-C. Hsieh, A. Maruyama, Y. Kitazumi, O. Shirai, K. Kano, *Sens. BioSensing Res.* **2015**, *5*, 90–96.
- [104] K. Sakai, Y. Kitazumi, O. Shirai, K. Kano, *Electrochemistry Communications* **2016**, *65*, 31–34.
- [105] K. Sakai, Y. Kitazumi, O. Shirai, K. Takagi, K. Kano, *Electrochemistry Communications* **2016**, *73*, 85–88.
- [106] S. S. Reginald, M. Etzerodt, D. Fapyane, I. S. Chang, *ACS Sens* **2021**, *6*, 2772–2782.
- [107] J. Alvarez-Malmagro, A. R. Oliveira, C. Gutiérrez-Sánchez, B. Villajos, I. A. C. Pereira, M. Vélez, M. Pita, A. L. De Lacey, *ACS Appl. Mater. Interfaces* **2021**, *13*, 11891–11900.
- [108] A. Heller, *Curr. Opin. Chem. Biol.* **2006**, *10*, 664–672.
- [109] R. Gracia, D. Mecerreyes, *Polym. Chem.* **2013**, *4*, 2206.
- [110] A. Ruff, *Curr. Opin. Electrochem.* **2017**, *5*, 66–73.
- [111] N. Plumeré, O. Rüdiger, A. A. Oughli, R. Williams, J. Vivekananthan, S. Pöller, W. Schuhmann, W. Lubitz, *Nat. Chem.* **2014**, *6*, 822–827.
- [112] H. Li, D. Buesen, S. Dementin, C. Léger, V. Fourmond, N. Plumeré, *J. Am. Chem. Soc.* **2019**, *141*, 16734–16742.
- [113] V. Fourmond, C. Léger, *ChemElectroChem* **2021**, *8*, 2607–2615.
- [114] C. Cadoux, R. D. Milton, *ChemElectroChem* **2020**, *7*, 1974–1986.
- [115] M. Yuan, S. Sahin, R. Cai, S. Abdellaoui, D. P. Hickey, S. D. Minter, R. D. Milton, *Angew. Chem. Int. Ed Engl.* **2018**, *57*, 6582–6586. *Angew. Chem.* **2018**, *130*, 6692–6696.
- [116] S. K. Kuk, K. Gopinath, R. K. Singh, T.-D. Kim, Y. Lee, W. S. Choi, J.-K. Lee, C. B. Park, *ACS Catal.* **2019**, *9*, 5584–5589.
- [117] J. Szczesny, A. Ruff, A. R. Oliveira, M. Pita, I. A. C. Pereira, A. L. De Lacey, W. Schuhmann, *ACS Energy Lett.* **2020**, *5*, 321–327.

## Graphical abstract



Only two enzymes are able to directly reduce CO<sub>2</sub>: the metalloenzymes formate dehydrogenase, which produces formate, and CO dehydrogenase, which produces carbon monoxide. We review the studies in which these enzymes were connected to electrodes, either for applicative purposes or to learn about their catalytic mechanism.